CHAPTER V

TRANSCRIPTOME ANALYSIS REVEALS JEJUNAL MECHANISMS UNDERLYING POSTBIOTIC LIC37 MEDIATED IMMUNE SYSTEM IN CALVES

5.1 Abstract

Weaning is a challenging for dairy calves, frequently resulting in digestive issues. This highlights the importance of implementing appropriate nutritional strategies to enhance gut health and support optimal growth. Postbiotics is a promising alternative to traditional probiotics by conferring health benefits without the risks associated with live bacteria. This study aimed to investigate the effect of dietary supplementation with postbiotic from heat killed *Limosilactobacillus ingluviei* C37 (postbiotic LIC37) on blood biochemical parameters, and jejunal epithelium transcriptomic profiles in calves. Results indicated that heat killed *Limosilactobacillus ingluviei* C37 supplementation reduced globulin, total protein, Neutrophil (Neu) and NLR levels in the TRT group ($P < 0.05$). Transcriptomic analysis identified 76 DEGs, with significant upregulation of genes involved in fatty acid metabolism (FABP1), intestinal barrier function (B4GALNT2), and detoxification (GSTA1), alongside downregulation of immune response regulation (FCRLA, FCRL4). Gene Ontology (GO) and Kyoto Encyclopedia of Genes and Genomes (KEGG) analyses highlighted enrichment in pathways related to Glutathione metabolism, Drug metabolism, and Vitamin digestion, indicating postbiotic LIC37 supplementation improved detoxification, oxidative stress defense, and nutrient absorption in calves. This study provides novel insights into the molecular mechanisms underlying the benefits of postbiotic LIC37 and supports their potential as a sustainable alternative to probiotics in calf nutrition.

Keywords: Calf weaning; Differentially expressed gene; Jejunal epithelium; *Limosilactobacillus*; Postbiotic; Transcriptome.

5.2 Introduction

Weaning is a particularly stressful and difficult event for dairy calves, which can easily cause intestinal disorders, with a high prevalence primarily attributed to developmental factors during the early postnatal stages. Specifically, gut immaturity, immune underdevelopment, and pathogen exposure primarily increase early life intestinal disease risk (Lopez and Heinrichs, 2022). Moreover, intestinal disorders not only compromise calf health; it also adversely affect weaning weights and subsequent milk yields (Aghakeshmiri et al., 2017). Hence, ensuring intestinal health is key to maximizing both growth potential and production performance.

Dietary intervention could offer novel approaches to ameliorate inflammatory disorders by modulating the immune response through metabolic rewiring. For decades, probiotics have been a staple in animal feed as additives to improve intestinal health (Mahesh et al., 2021). Yet, the widespread presence of antibiotic resistance genes in these strains, and the demonstrated ability for these genes to transfer between organisms (Marteau and Shanahan, 2003), casts a long shadow over their suitability for continued use as live bacteria in future nutritional strategies. Offering a compelling alternative to traditional probiotics, postbiotics are defined as a “preparation of inanimate microorganisms and/or their components that confers a health benefit on the host” (Salminen et al., 2021), which could enhance host antioxidant capacity and immunity, regulate gut microbiota, and thereby support intestinal health. For example, Izuddin et al. (2019) found that feeding lambs with postbiotic from metabolites of *Lactobacillus plantarum* RG14 could improve growth performance, and nutrient intake; Feng et al. (2022) demonstrated that the profound effects of postbiotic from *Bifidobacterium bifidum* B1628 on alleviating inflammation and intestinal damage in murine models.

RNA sequencing (RNA-Seq) is widely utilized to examine transcriptomic changes in key tissues in response to various intrinsic and extrinsic factors, offering insights into gene regulation and physiological adaptations (Kim et al., 2022). Currently, RNA-Seq studies in ruminant nutrition mainly focus on the rumen (Zhao et al., 2017), colon (Jin et al., 2024), and liver (Fernandes et al., 2024), while studies investigating the jejunal epithelium in calves are relatively scarce.

5.3 Objective

This study aimed to conducted RNA-seq on the jejunal epithelium of calves to identify differential gene expression (DEGs) and uncover the underlying molecular mechanisms associated with a postbiotic from heat killed *Limosilactobacillus ingluviei* C37 supplemented diet.

5.4 Materials and methods

5.4.1 Ethics statement

The experiments were carried out at the Suranaree University of Technology (SUT) farm according to the approved protocol by the Animal Care and Use Committee of SUT, Thailand (document no. (SUT-IACUC-0020/2023).

5.4.2 Treatments, and management

The *Limosilactobacillus ingluviei* C37 strain (*L. ingluviei* C37) was sourced by the Laboratory of Monogastric Animal Nutrition and Feed Science at Suranaree University of Technology (SUT). The isolation and culture of *L. ingluviei* C37 was described in detail by report of Sirisopapong et al. (2023). The inactivated *L. ingluviei* C37 was prepared by heat-killed at 80°C for 30 min according to the method of Tsukagoshi et al. (2020).

Fourteen Holstein bull calves were collected from a single farm within one week of birth. The calf received 2 liters of colostrum within 3 hours of birth, and an additional 2 liters within the subsequent 12 hours. At 24 hours after birth, the serum total protein was using a Brix refractometer (Lohand Bio Co. Ltd. Hangzhou, China) to ensure an effective transfer of passive immunity (Hernandez et al., 2016), the calf with serum total protein greater than 5.6 g/dL was selected. Subsequently, the transition from colostrum feeding to bucket-fed milk replacer (MR) begins at 3 days of age, then transferred to the SUT farm. All calves received an intramuscular injection of 5% (v/w, mL/kg) vitamin B_{12} (Catosal^{TM}, OLIC Co. Ltd, Ayutthaya, Thailand) upon their arrived. Commercial MR was procured from Dairy-Rich Co. Ltd (Bangkok, Thailand). One kilogram of MR contained 974 g dry matter, 88.7 g ash, 226.7 g crude protein, and 177.4 g fat.A total of fourteen calves (33.69 ± 5.28 kg; mean ± SD) with similar age (5.71 ± 1.14 d; mean ± SD) were selected and randomly assigned to two groups (7 per group), including 1 control group (without postbiotic LIC37), and 1 treatment group with 1g postbiotic LIC37 (10^8 CFU/g). The dose was converted based on previous studies (Thorsteinsson et al., 2020; McNeil et al., 2024). Each calf was housed in an individual pen (2.2 m × 2.4 m) with rubber mats and wood pellets on the floor. The contaminated wood pellets were cleaned daily, and the wood pellets were replaced weekly.

MR was fed daily at a concentration of 15% at 1.75% body weight (BW) (air-dry basis) at 08:00 and 16:00. MR was adjusted weekly for BW. The postbiotic LIC37 was mixed with MR during the morning feeding, and cleanly water was available *ad libitum*. As the sole solid feed, the commercial starter (Charoen Pokphand Foods, Bangkok, Thailand) was provided *ad libitum* from day 33 of the experiment. One kilogram of starter contained 909.4 g dry matter, 89.7 g ash, 237.9 g crude protein, 39.9 g fat, 520.9 g of neutral detergent fiber, and 122.4 g acid detergent fiber.

The experiment spanned 90 days, with the calves' arrival day considered as day 1. Daily recording of MR and starter intake, and measured BW weekly. The milk replacer was adjusted according to BW weekly. Calves began the weaning step-down at d 82, with the MR solution being restricted to 50% of the previous week's allocation. Calves were completely weaned by d 90. This feeding regimen was designed to elicit weaning stress (Van Niekerk et al., 2021).

5.4.3 Sampling method

On d 76 (pre-weaning), 83 (mid-weaning), and 90 (post-weaning), respectively. Prior to the morning feeding, blood samples were collected by jugular venipuncture using sterile tube without anticoagulation. Then, transferred to the SUT hospital detecting serum biochemical parameters, which encompassed total protein, globulin, albumin, and complete blood count.

On the last day of the experimental period (d 90), prior to morning feeding. Four calves were randomly selected from each group and euthanized using captive bolt stunning and exsanguinated. The abdominal cavity was quickly opened. The jejunum was defined as starting at 100 cm caudal to the pylorus. Jejunal samples were collected approximately 30 cm proximal to the collateral branch of the cranial mesenteric artery, rinsed three times with sterile phosphate-buffered saline (PBS, pH = 7.0), and immediately placed into sterile RNase-free tubes. The samples were then flash-frozen in liquid nitrogen and stored at -80°C until RNA extraction.

5.4.4 Library construction and data processing

Construction of the cDNA library and RNA-seq were performed by BGI Co. Ltd. (BGI, Shenzhen, China). Six libraries were tested on the DNBSEQ platform. Sequencing data were filtered using SOAPnuke Version v1.5.6 (Cock et al., 2010). Reads containing adapters, reads with unknown base N content greater than 5%, and low-quality reads (reads with a base quality value less than 15 accounting for more than 20% of the total base number of the reads) were removed to obtain clean reads. Subsequently, we used HISAT2 v2.1.0 (Kim et al., 2015) to align the clean reads to the chicken reference genome (GCF_000002315.6_GRCg6a) and then used RSEM Version v1.3.1 (Li and Dewey, 2011) to align the clean reads to the reference gene set.

5.4.5 RNA extraction and RNA-seq library construction

Total RNA was extracted from jejunal epithelium using TRIzol reagent (Molecular Research Center, Cincinnati, OH, USA) according to the manufacturer's instructions. The quality and quantity of the extracted RNA were analysis using spectrophotometry (NanoDrop 2000 spectrophotometer; Thermo Fisher Scientific, Waltham, MA) and 1% agarose (w/v) gel electrophoresis with 0.5 × TAE as a buffer and an electric current of 100 V for 20 min. The RNA integrity numbers (RIN) was determined by the capillary electrophoresis with a QIAxcel Connect, all the samples with RIN greater than 6.5 were used to construct the sequencing library.

RNA reverse transcription, library preparation, and RNA sequencing (RNA-seq) were conducted at BGI Co., Ltd. (Shenzhen, China). In brief, total RNA was subjected to mRNA with poly(A) enrichment using oligo(dT) magnetic beads for reverse transcription and cDNA synthesis. The double stranded cDNA underwent end repair, 5'-phosphorylation, and 3'-adenylation to facilitate adapter ligation. Adapter ligated products were PCR amplified, denatured, and circularized using bridging primers to construct single stranded circular DNA libraries. The sequencing was performed using the DNBSEQ platforms with PE500 (BGI Co. Ltd., Shenzhen, China).

The raw sequencing data were processed using SOAPnuke (v1.5.6, RRID:SCR_015025) to remove low-quality and adapter-contaminated reads. The reads were filtered based on the following criteria: 1) reads containing adapter sequences (adapter contamination), 2) reads with unknown bases (N) exceeding 5% of the total bases, and 3) low-quality reads (defined as reads where more than 20% of the bases had a quality score below 15).

5.4.6 Transcriptome sequencing and data analysis

The resulting high-quality reads were retained as clean data and subsequently analyzed using the online multi-omics data mining system (biosys.bgi.com). In brief, the data were aligned to the reference *Bos taurus* genome (GeneBank Assembly ID: GCA_002263795.2) using HISAT2 version 2.2.1 (Kim et al., 2015) with default parameters. The clean data were aligned to the reference gene set using Bowtie version 2.3.4.3 (Langmead and Salzberg, 2012). The RSEM version 1.3.1 (Li and Dewey, 2011) was used to perform gene expression quantification. Differential expression analysis between the two groups was performed using DESeq2 version 1.4.5 (Love et al., 2014). The differential genes with a fold-change (FC) of ≥ 1 and an adjusted P value < 0.05 were classified as differentially expressed genes (DEGs). The Phyper program in R software was used to conduct Gene Ontology (GO) annotation and Kyoto Encyclopedia of Genes and Genomes (KEGG) pathway enrichment analyses of DEGs. The GO terms and KEGG pathways with $P < 0.05$ were considered significantly enriched. All sequencing data have been deposited in the Gene Expression Omnibus (GEO) of the National Center for Biotechnology Information (NCBI) database under the accession number GSE293812.

5.4.7 Validation by real-time PCR

The RNA was transcribed into complementary DNA (cDNA) with the SweScript All-in-One RT SuperMix (G3337, Servicebio Technology Co., Ltd., Wuhan, China), following the manufacturer's guidelines. Primers were designed using Primer3 software (https://primer3.ut.ee/) and synthesized by Servicebio Technology Co., Ltd. (Wuhan, China) (**Table 5.1**). A total of 7 were selected DEGs in the same RNA samples were evaluated by quantitative polymerase chain reaction (qPCR) to verify the reliability and reproducibility of RNA-seq. These DEGs were Beta-1,4-N-Acetyl-Galactosaminyl transferase 2 (B4GALNT2), Fatty Acid Binding Protein 1 (FABP1), Glutathione S-Transferase Alpha 1 (GSTA1), Paired Box 9 (PAX9), Paired Box 5 (PAX5), Fc Receptor Like 4 (FCRL4), and Fc Receptor Like A (FCRLA). The qPCR was carried out on the CFX Connect™ Real-Time PCR System (Bio-Rad, California, USA) using a 15 μL reaction mixture containing 2 μL of cDNA, 1.5 μL of each primer (10 μM), 7.5 μL of 2× Universal Blue SYBR Green qPCR Master Mix (G3326, Servicebio Technology Co., Ltd., Wuhan, China), and 4 μL of nuclease-free water. The thermal cycling protocol included an initial denaturation at 95°C for 30 seconds, followed by 40 cycles of denaturation at 95°C for 15 seconds, annealing at 60°C for 15 seconds, and extension at 60°C for 30 seconds. Relative gene expression was quantified using the $2^{-\Delta\Delta CT}$ method (Love et al., 2014), with Glyceraldehyde-3-phosphate dehydrogenase (GAPDH) as an internal reference. The results converted into fold change (FC) values for comparison with RNA-Seq data.

Table 5.1 Primer sequences used in quantitative PCR.

Gene	Primer sequences	Accession No.
B4GALNT2	(F): TGA CCA ACT TCG CCA GAA CA	508108
	(R): TTC CGC TCT GTT GAA ACG GT	
FABP1	(F): GTA CCA AGT CCA GAC CCA GG	327700
	(R): GAT TTC CGA CAC CCC CTT GAT	
GSTA1	(F): GGA GAC AGA CTT TCG TAA GGA TTG A	777644
	(R): ATC TTT TTC AGC AGG TGG GCA	
PAX9	(F): GTG GTC CCA ACA CTC CCT TT	540196
	(R): CAT GAT TCA CCG AGA GCC CA	
PAX5	(F): CGA AGA ACA CGG ACA CCC TT	538371
	(R): AAG AGC TTC TCG CCA TGT GA	
FCRL4	(F): CCA GAC ACT CGG CTT CAC TT	534753
	(R): CAG TGT TTC AGC ACC ACA CG	
FCRLA	(F): AGC AGC CAC TGA GGA CAA TC	782871
	(R): CTA ACA GTA TAC CAG GGG CAG T	

Abbreviations: B4GALNT2, Beta-1,4-N-Acetyl-Galactosaminyltransferase 2; FABP1, Fatty Acid Binding Protein 1; GSTA1, Glutathione S-Transferase Alpha 1; PAX9, Paired Box 9; PAX5, Paired Box 5; FCRL4, Fc Receptor Like 4; FCRLA, Fc Receptor Like A.

5.4.8 Data and statistical analysis

Normally of data distribution was confirmed using the Shapiro-Wilk procedure of SPSS (version 27, Chicago, IL, USA). The data on plasma biochemical parameters were analyzed using the General Linear Model (GLM) in SPSS to analyze variables that were repeatedly measured over time. Sphericity was assessed using Mauchly's test, with the Greenhouse-Geisser correction applied whenever the assumption was breached. The significance level was set a P value < 0.05.

5.5 Results

5.5.1 Quality of RNA-seq reads

A comparative RNA-seq analysis was performed on the jejunal epithelium transcriptome to evaluate the effects of postbiotic LIC37 supplementation on the transcriptomic profile of the jejunal epithelium in calves. The RNA-seq results for jejunal epithelium samples are presented in **Table S5.1**. The raw data reads ranged from 45.44 million to 47.19 million, with an average of 46.10 million reads. After filtering out low-quality reads, contamination, and other artifacts from the raw data, the number of clean reads ranged from 43.87 million to 45.15 million, with an average of 44.43 million. The GC content of clean reads varied from 49.26% to 52.10%, averaging 50.52%. Additionally, at least 95.70% of the reads had a sequence quality score greater than Q30 (percentage of bases with a Phred value ≥ 30). High-quality reads were mapped to the reference genome at a ratio of 97.11% to 98.04%, with an average of 97.53%.

5.5.2 DEGs Analysis

Eight cDNA libraries were constructed to identify DEGs associated with the postbiotic LIC37 response in the jejunum. As illustrated in **Figure 5.1**, a total of 76 DEGs were identified, comprising 36 upregulated and 40 downregulated genes.

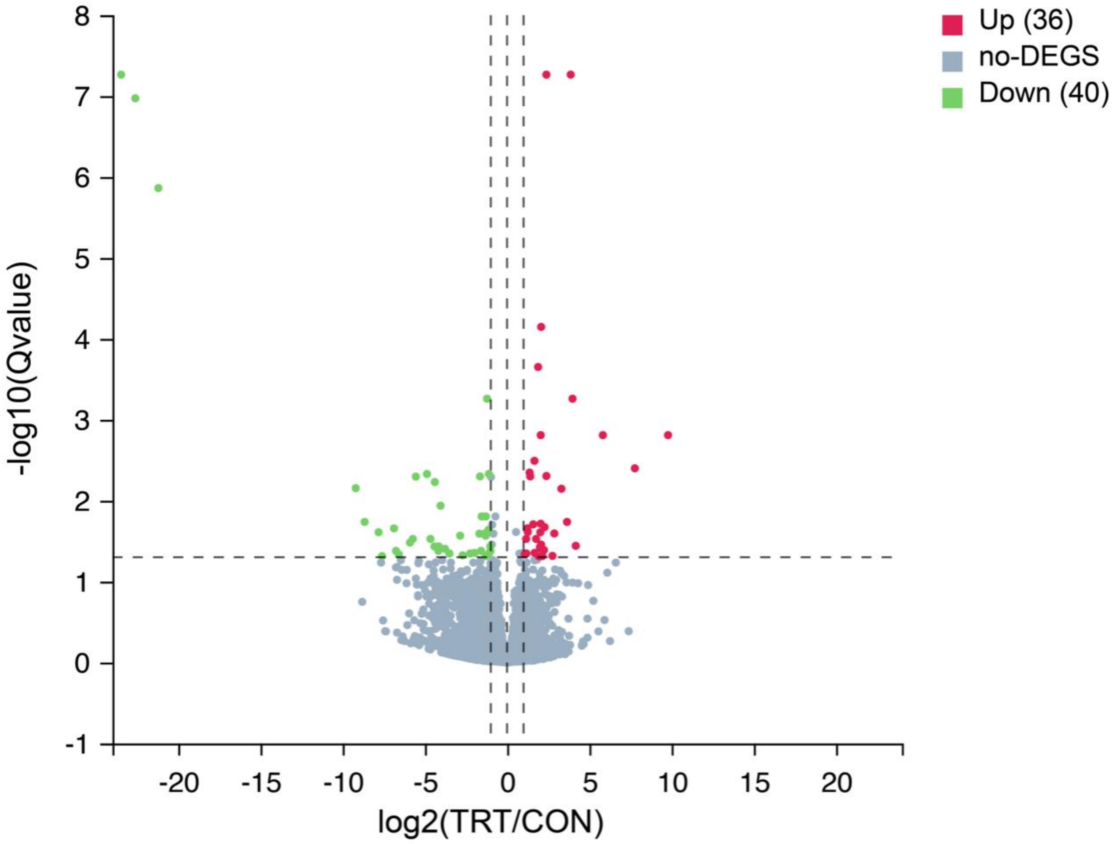

Figure 5.1 Volcano plot of differentially expressed genes in the jejunal tissue of calves. The genes meeting the conditions of adjusted P (Q value) < 0.05 and |log2 FC| ≥ 1 are considered as significant differentially expressed genes (DEGs), with red and green dots representing upregulated and downregulated transcripts, respectively. Gray dots represent insignificant DEGs. The x and y axes of the volcano plots show the log2 fold changes and –log10 q value, respectively.

The genes related to metabolism and immunity were regulated by postbiotic LIC37 supplementation, such as Fatty Acid Binding Protein 1 (FABP1), and Glucosylceramidase Beta 3 (GBA3). Additionally, the genes associated with intestinal barrier and immunity, such as Beta-1,4-N-Acetyl-Galactosaminyltransferase 2 (B4GALNT2), Glutathione S-Transferase A1 (GSTA1), and One Cut Homeobox 2 (ONECUT2). On the other hand, the genes associated with inflammation showed a downregulation, such as Paired Box 5 (PAX5), Paired Box 9 (PAX9,), Fc Receptor Like A

(FCRLA), and Fc Receptor Like 4 (FCRL4). The top 20 upregulated and top 20 downregulated DEGs were presented in **Table 5.2**.

Table 5.2 Top 20 upregulated and downregulated differentially expressed genes affected by postbiotic LIC37 supplementation in the jejunal tissue of calves.

Gene ID	Symbol[1]	Log2 fold change	Qvalue[2]	Regulated
508108	B4GALNT2	9.7874	1.55E-03	Up
327700	FABP1	7.7692	3.97E-03	Up
539625	GBA3	5.8228	1.55E-03	Up
786706	-	4.1697	3.61E-02	Up
777644	GSTA1	3.9776	5.49E-04	Up
539937	ARL14	3.8660	5.44E-08	Up
782542	ONECUT2	3.6487	1.83E-02	Up
511869	TM4SF5	3.2932	7.12E-03	Up
505865	FOLH1B	2.8627	2.54E-02	Up
538670	FAM151A	2.7599	4.83E-02	Up
414732	GATM	2.3843	4.97E-03	Up
525682	NOTUM	2.3823	5.44E-08	Up
786760	BTN3A3	2.2747	2.13E-02	Up
514667	MST1	2.2436	4.08E-02	Up
100336768	ROS1	2.1404	4.85E-02	Up
407225	MOGAT1	2.0725	3.49E-02	Up
511097	SLC46A1	2.0696	7.13E-05	Up
100300004	GLTPD2	2.0471	1.55E-03	Up
282605	FAM13A	2.0424	1.92E-02	Up

Table 5.2 Continue.

Gene ID	Symbol[1]	Log2 fold change	Qvalue[2]	Regulated
513137	TMEM72	2.0322	3.76E-02	Up
540196	PAX9	-23.4653	5.44E-08	Down
112444345	-	-22.6113	1.07E-07	Down
112446673	-	-21.2060	1.37E-06	Down
538371	PAX5	-9.2089	6.98E-03	Down
534753	FCRL4	-8.6701	1.83E-02	Down
782871	FCRLA	-7.8139	2.45E-02	Down
531420	GP2	-7.6012	4.85E-02	Down
504258	SIGLEC10	-6.8829	2.20E-02	Down
407126	CR2	-6.7550	4.18E-02	Down
107131854	-	-6.5830	4.60E-02	Down
408008	KCNN1	-5.9122	3.30E-02	Down
512439	HBA	-5.7393	2.97E-02	Down
112445446	-	-5.5555	5.03E-03	Down
493988	SLC14A1	-4.8759	4.67E-03	Down
101908107	P2RY8	-4.6693	2.97E-02	Down
515911	STRA6	-4.4179	3.68E-02	Down
782922	-	-4.3880	5.88E-03	Down
616320	SLC9B2	-4.1830	4.18E-02	Down
100296105	-	-4.1574	3.68E-02	Down
506550	TSPAN1	-4.0508	1.16E-02	Down

[1] B4GALNT2, Beta-1,4-N-Acetyl-Galactosaminyl transferase 2; FABP1, Fatty Acid Binding

Protein 1; GBA3, Glucosylceramidase Beta 3; GSTA1, Glutathione S-Transferase Alpha 1; ARL14, ADP Ribosylation Factor Like GTPase 14; ONECUT2, One Cut Homeobox 2; TM4SF5, Transmembrane 4 L Six Family Member 5; FOLH1B, Folate Hydrolase 1B; FAM151A, Family with Sequence Similarity 151 Member A; GATM, Glycine Amidino transferase; NOTUM, Notum, Palmitoleoyl-Protein Carboxylesterase; BTN3A3, butyrophilin subfamily 3 member A3; MST1, Macrophage Stimulating 1; ROS1, Receptor Tyrosine Kinase 1; MOGAT1, Monoglyceride O-acyltransferase 1; SLC46A1, Solute Carrier Family 46 Member 1; GLTPD2, GLTP Domain Containing 2; FAM13A, Family with Sequence Similarity 13 Member A; TMEM72, Transmembrane Protein 72; PAX9, Paired Box 9; PAX5, Paired Box 5; FCRL4, Fc Receptor Like 4; GP2, Glycoprotein 2; FCRLA, Fc Receptor Like A; GP2, Glycoprotein 2; SIGLEC10, Sialic Acid Binding Ig-like Lectin 10; CR2, Complement Receptor 2; KCNN1, Potassium Channel, Calcium Activated, Subfamily N, Member 1; HBA, Hemoglobin Subunit Alpha; SLC14A1, Solute Carrier Family 14 Member 1; P2RY8, Purinergic Receptor P2Y8; STRA6, Stimulated by Retinoic Acid 6; SLC9B2, Solute Carrier Family 9 Member B2; TSPAN1, Tetraspanin 1.

[2] Q value is adjusted P value.

5.5.3 GO and KEGG enrichment analysis of DEGs

GO and KEGG pathway analyses were performed on the 76 identified DEGs. The GO analysis classified these DEGs into three categories: biological processes (BP), molecular functions (MF), and cellular components (CC). A total of 352 enriched GO terms were identified. In the BP category, 152 GO terms were significantly enriched. The five most significant GO terms included mitral valve formation (P = 4.39E-05), positive regulation of metallopeptidase activity (P = 8.76E-05), prostaglandin metabolic process (P = 3.88E-04), reproductive process (P = 4.05E-04), and post-anal tail morphogenesis (P = 0.0017). For the MF category, 53 GO terms showed significantly enriched. Among these, the top five GO terms were transmembrane signaling receptor activity (P = 0.0065), actin filament binding (P = 0.0038), molecular function (P = 0.0200), extracellular matrix structural constituent (P = 0.0013), and peroxidase activity (P = 0.0084). In the CC category, 20 GO terms were significantly enriched. The top five most significant GO terms included membrane (P = 0.0031), cellular component (P = 0.014), integral component of Golgi membrane (P = 0.0164), extracellular space (P = 0.0165), and integral component of plasma membrane (P = 0.0189). **Figure 5.2** presents the 20 most significantly enriched GO terms.

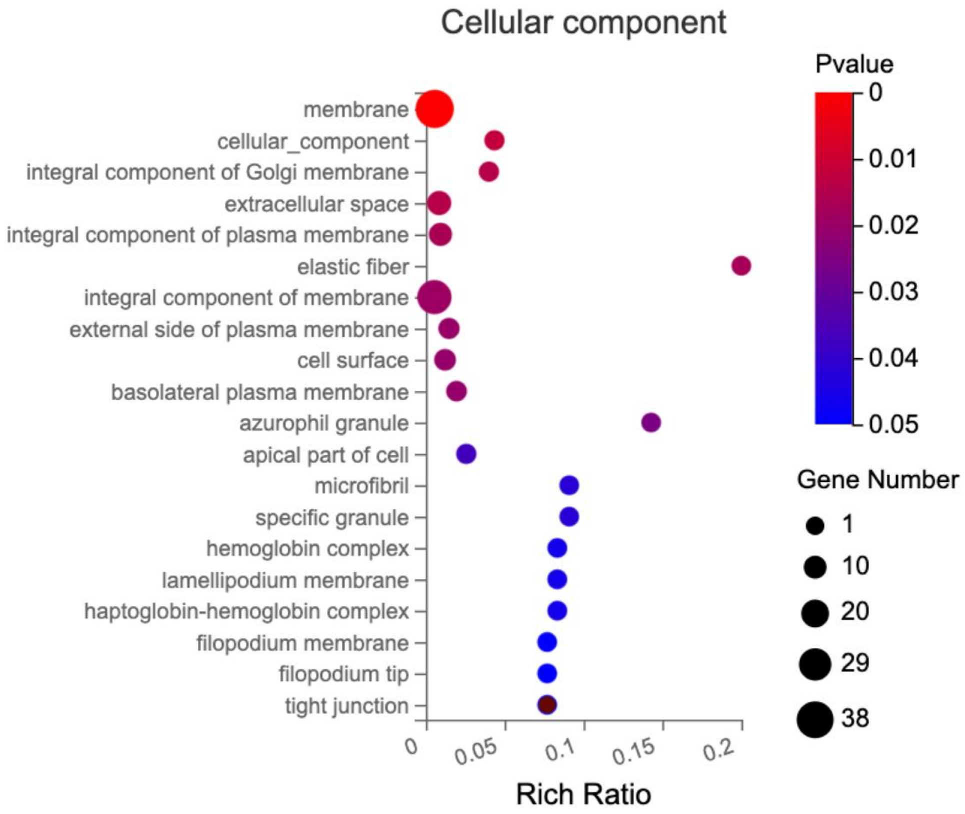

Figure 5.2 Top 20 GO cellular component terms enriched in differentially expressed genes in jejunal epithelium in calves. The circle size in each term corresponds to the number of genes. The circle's color goes from blue to red, indicating a lower P value.

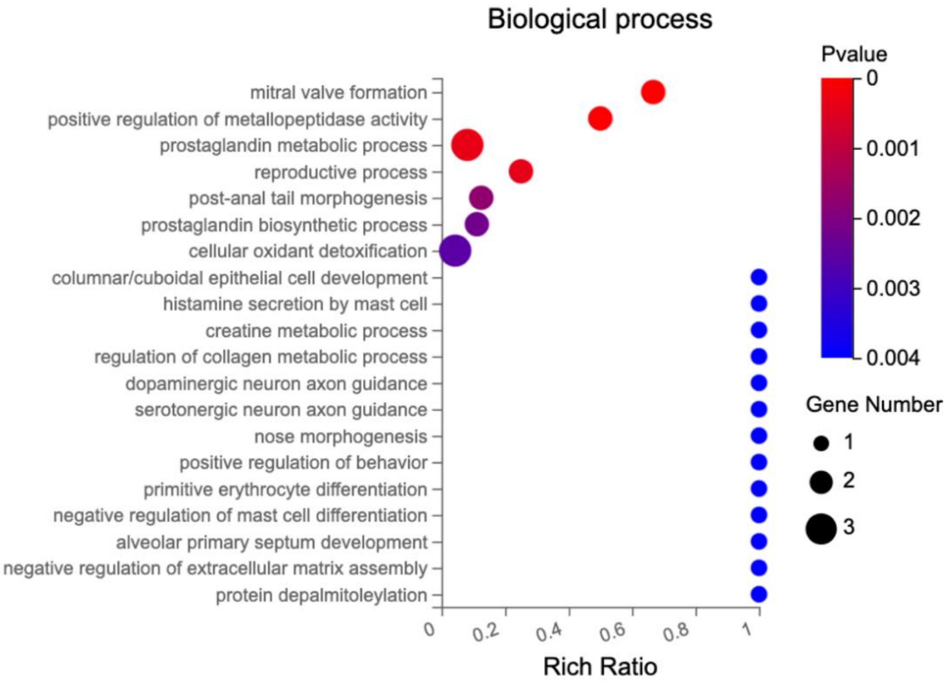

Figure 5.3 Top 20 GO biological process terms enriched in differentially expressed genes in jejunal epithelium in calves.

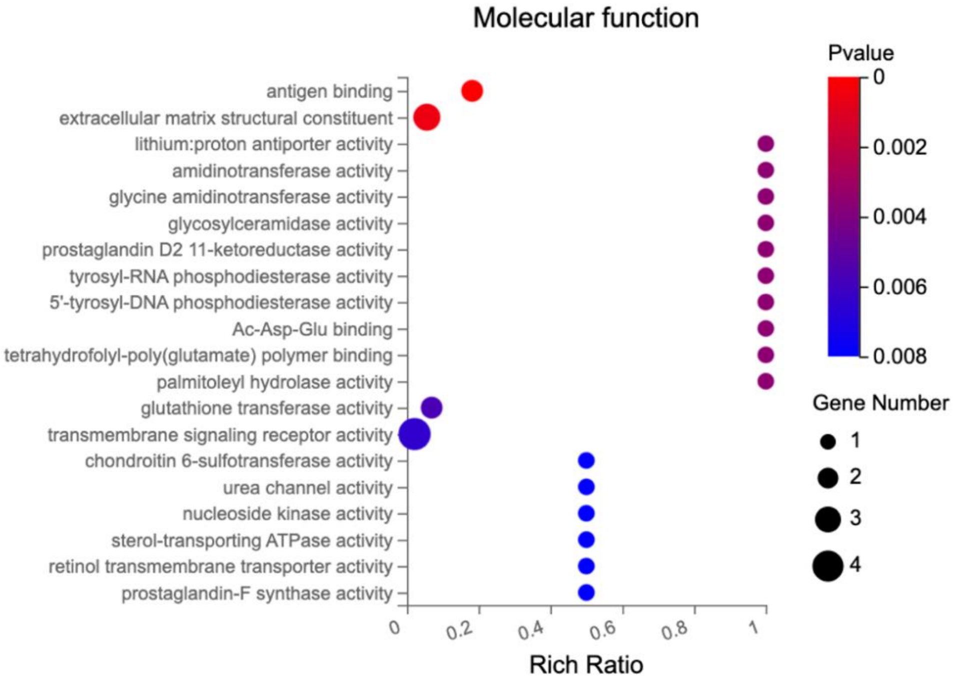

Figure 5.4 Top 20 GO molecular function terms enriched in differentially expressed genes in jejunal epithelium in calves.

KEGG pathway analysis of the jejunal epithelial tissue identified 8 significantly enriched pathways, namely Arachidonic acid metabolism (P = 0.0045), Drug metabolism - other enzymes (P = 0.0020; bta00983), Vitamin digestion and absorption (P = 0.0036; bta04977), Glutathione metabolism (P = 0.0182; bta00480), Drug metabolism - cytochrome P450 (P = 0.0182; bta00982), Chemical carcinogenesis - DNA adducts (P = 0.0199; bta05204), Metabolism of xenobiotics by cytochrome P450 (P = 0.0211; bta00980), Hepatocellular carcinoma (P = 0.0198; bta05225), and Platinum drug resistance (P = 0.0280; bta01524). **Figure 5.3** presents the 20 most enriched KEGG pathways.

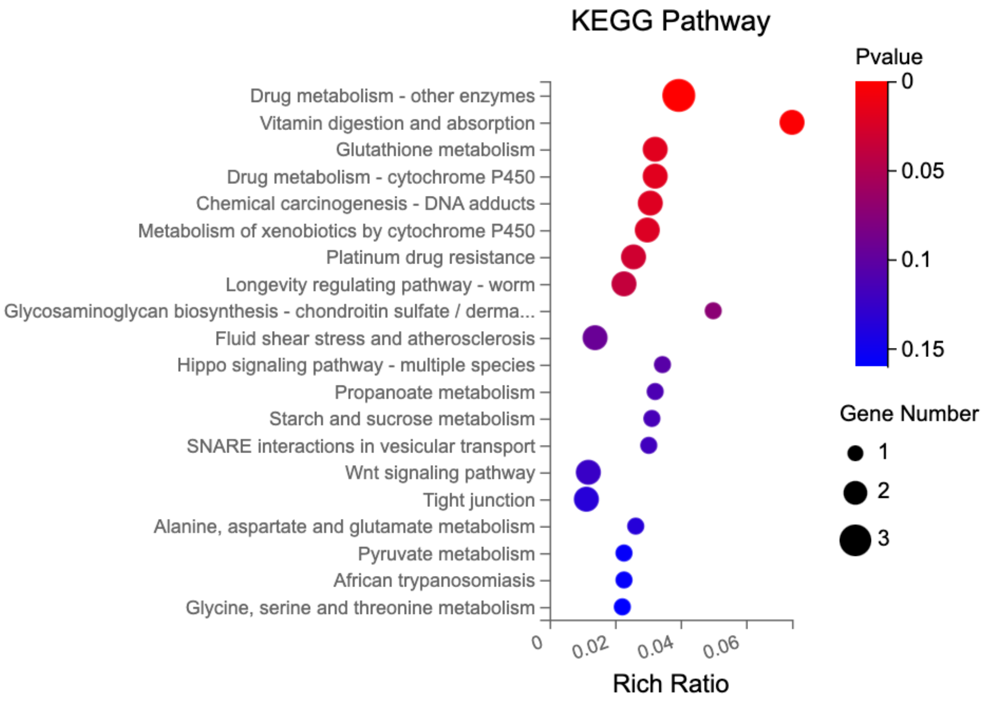

Figure 5.5 Top 20 enriched KEGG pathway of differentially expressed genes in jejunal tissue of calves. The circle size in each term corresponds to the number of genes. The circle's color goes from blue to red, indicating a lower P value.

5.5.4 Validation of RNA-seq results by quantitative PCR

To validate the RNA-seq results, we selected a subset of DEGs for qPCR analysis. Specifically, the expression levels of seven DEGs, including three upregulated genes (e.g. B4GALNT2, FABP1, and GSTA1) and four downregulated genes (e.g. PAX9, PAX5, FCRL4, and FCRLA), were quantified in jejunal tissue. The qPCR results exhibited expression patterns consistent with the RNA-seq data, confirming the reliability and accuracy of our transcriptomic analysis (**Figure 5.4**).

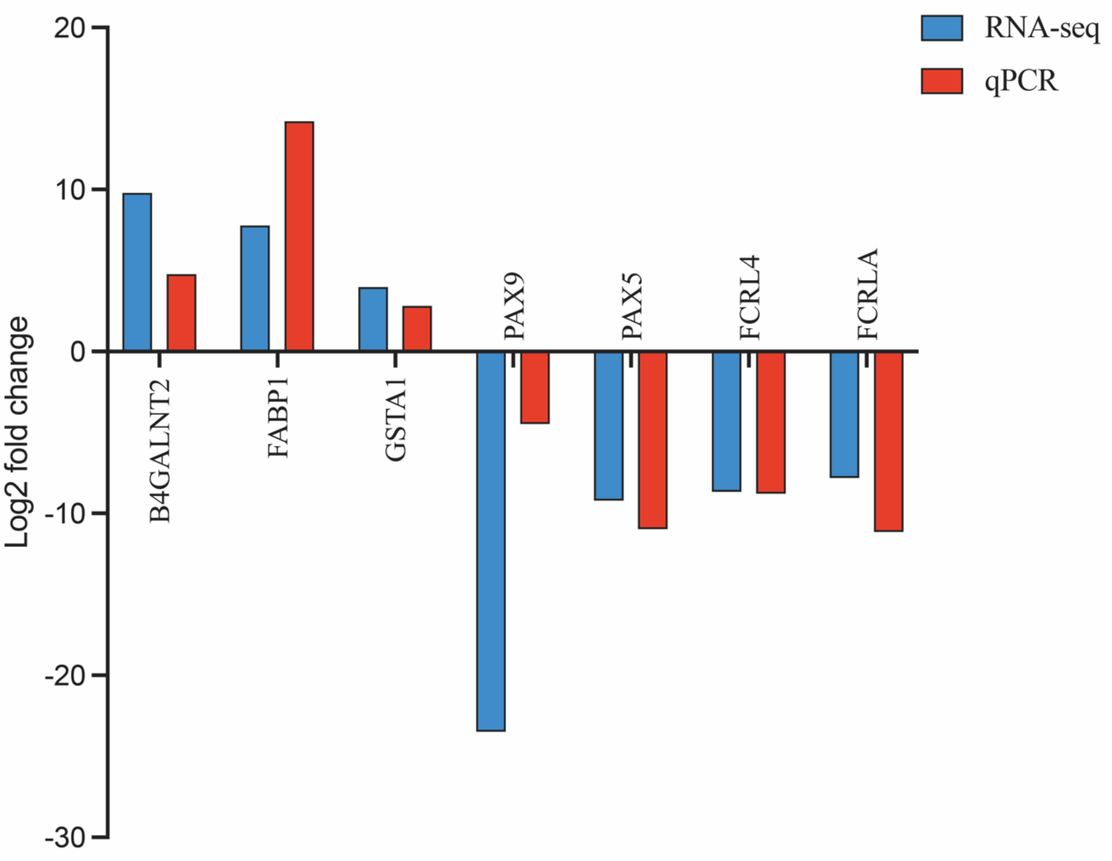

Figure 5.6 Quantitative PCR (qPCR) was employed to validate five DEGs in RNA-seq analysis. The x-axis denotes the genes, while the y-axis shows their mRNA expression levels as fold-change (FC) values. Expression levels obtained from RNA-seq and qPCR are illustrated by blue and red bars, respectively. B4GALNT2, Beta-1,4-N-Acetyl-Galactosaminyl transferase 2; FABP1, Fatty Acid Binding Protein 1; GSTA1, Glutathione S-Transferase Alpha 1; PAX9, Paired Box 9; PAX5, Paired Box 5; FCRL4, Fc Receptor Like 4; FCRLA, Fc Receptor Like A.

5.6 Discussion

In ruminants, the rumen is not fully developed before weaning, making the small intestine the primary organ responsible for nutrient absorption and immune function (Song et al., 2021). A major function of the intestinal epithelium is to transport and present dietary and bacterial antigens to the immune system (Kelly and Coutts, 2000). The transcriptome of the small intestinal epithelium may provide insights into key genes involved in the regulation of nutrient metabolism and immune function. Postbiotics consist of metabolites such as bacteriocins, peptides, organic acids, and volatile compounds, which display antioxidant and antimicrobial properties (Vasiee et al., 2020; Amiri et al., 2022). Furthermore, they may aid in preventing pathogen adhesion to the gut (Reuben et al., 2020), thereby acting as protectors of intestinal health. In the present study, we identified multiple genes associated with immune response and inflammation, metabolism and detoxification, and cellular signaling.

Of which, FABP1 was highly expressed in bovine jejunal epithelial and involved in fatty acid metabolism (Hayashi et al., 2013), which exerts a cytoprotective role by binding toxic molecules like free fatty acids and heme (Wang et al., 2015), while its antioxidant activity, driven by methionine and cysteine residues, helps reduce reactive oxygen species (ROS) production (Yan et al., 2009). Previous studies have reported that downregulated expression of the FABP1 in the intestine of broilers under stress, such as heat stress (Habashy et al., 2017), and high stocking density (Elbaz et al., 2024a). Consistent findings have reported in monogastric animals. For instance, Wang et al. (2021) reported that feeding broilers with *Lactobacillus plantarum* 16 significantly upregulated mRNA expression of FABP1 in the ileal mucosa, which resulted in better transport and absorption of nutrients. Similarly, an increased expression of FABP1 and CAT1 genes were observed in ileal mucosa of broilers fed with *Bacillus subtilis* (Elbaz et al., 2024b). In the present study, we observed that FABP1 gene was significantly upregulated in the TRT group compared with the control group, suggesting that postbiotic LIC37 enhances FABP1 expression to bind toxic macromolecules while simultaneously inhibiting reactive oxygen species production, thereby providing comprehensive protection to intestinal epithelial cells. B4GALNT2, a glycosyltransferase responsible for synthesizing Sd(a)/Cad antigen-like structures (Byrne et al., 2018), which enhances intestinal barrier function, infection resistance, and immune homeostasis through glycosylation regulation, playing a crucial role in maintaining gut health (CAPON et al., 2001). In the present study, the expression of B4GALNT2 significantly upregulated in the TRT group with a 7.44 of fold change compared to the CON group. This upregulation was indicative of this postbiotic LIC37 promoting the synthesis of numerous carbohydrate structures required for building Sd(a)/Cad-antigen-like structures, which confer protection to the jejunal epithelium. Similarly, Jiang et al. (2023) reported that feeding lactating cows with *Saccharomyces cerevisiae fermentation product* upregulated expression of B4GALNT2, thereby enhancing the ileum's ability to defend against harmful molecules or microorganisms. We observed that postbiotic LIC37 supplementation leads to an upregulation of GBA3 expression in the jejunal epithelium of calves. GBA3 is an enzyme with broad substrate specificity, capable of hydrolyzing various plant-derived β-glucosides, including phenolic glucosides, cyanogenic glucosides, isoflavones, and flavones (Lopes-Marques et al., 2020). The upregulation of GBA3 indicates an enhanced capacity of the intestine to process dietary plant glucosides (Németh et al., 2003). These glucosides may be converted into more absorbable forms through hydrolysis and removal of their sugar moieties, thereby reducing their toxic effects on the host (Liu et al., 2017). These findings indicate that postbiotic LIC37 supplementation may promote the absorption of these nutrients and reduce their potential toxic impact on the host by upregulating GBA3, which enhances the intestinal detoxification and metabolic capacity for these dietary glucosides. GSTA1 exhibits GSH-dependent steroid isomerase activity as well as GSH-dependent selenium independent peroxidase activity (McIlwain et al., 2006), It has been demonstrated to protect cells from the detrimental effects of ROS-induced lipid peroxidation during oxidative stress induced by various factors (Yang et al., 2001). GSTA1 also protects cells by binding to GSH and mitigating oxidative stress, thereby reducing subsequent lipid peroxidation (Sharma et al., 2004). Additionally, a key function of GSTA1 is its role in inhibiting stress signaling kinases (JNK), which in turn influences the activation of caspases and the apoptosis cascade within the cell (Romero et al., 2006). A previous study reported that treatment with antioxidants can reduced the apoptosis of porcine enterocytes by up-regulating the expression of GSTA1 and regulating glutathione related redox homeostasis (Liu et al., 2018). Consistently, postbiotic LIC37 upregulated expression of GSTA1 in the jejunal epithelium of calves. This upregulation of GSTA1 may contribute to the protection of the intestinal epithelium by enhancing cellular antioxidant defenses and mitigating oxidative stress. Specifically, by increasing GSTA1 levels, postbiotic LIC37 supplementation may reduce oxidative damage, limit inflammation, and prevent cell apoptosis, ultimately supporting the integrity and function of the jejunal epithelium under stress conditions. In the present study, we observed that postbiotic LIC37 supplementation enhances the expression of ONECUT2 in the jejunal epithelium of calves. This finding is consistent with previous research indicating the crucial role of ONECUT2 in regulating cell proliferation, migration, adhesion, differentiation, and metabolism across various tissues such as the liver, pancreas, retina, neurons, and the immune system (Yu et al., 2020; Zhang et al., 2024). In particular, ONECUT2 has been shown to be essential for the development and differentiation of cells in these tissues. In ONECUT2 knockout mice, the lack of this gene led to failure to thrive during the critical period before weaning, with a 25-30% reduction in size and weight by postnatal day 19 and a higher mortality rate (only 70% survived before weaning) (Dusing et al., 2010). These findings highlight the importance of ONECUT2 in early development and suggest that postbiotic LIC37 supplementation may support the jejunal growth and differentiation of calves, potentially enhancing stress resistance during the weaning period. By upregulating ONECUT2, postbiotic LIC37 supplementation could contribute to the maintenance of intestinal barrier integrity, enhancing epithelial cell proliferation and differentiation, and reducing stress-related damage in the jejunum. Similarly, a reported by Jiang et al. (2023), who demonstrated that feeing lactating cows with *Saccharomyces cerevisiae* fermentation product showed a significant upregulated expression of ONECUT2 in ileal epithelium.

On the other hand, the expressions of PAX5 and PAX9 were downregulated by postbiotic LIC37 supplementation. PAX5 and PAX9 are members belonging to the Pax gene family, which are involved in regulating various biological processes (Blake and Ziman, 2014). Specifically, PAX5 has been shown to inhibit several biological activities of B cells, including cell-cell communication, cell adhesion, cellular metabolism, migration, and nuclear processes (Delogu et al., 2006). The downregulation of PAX5 may increase PTEN expression and inhibit the PI3K-AKT signaling pathway, thereby reducing the secretion of TNF-α and IL-6 (Calderón et al., 2021). Regarding PAX9, while its role has been primarily studied in skeletal development (Rodrigo et al., 2003; Borges et al., 2025), recent findings suggest a potential interaction between PAX9 and the NF-**K**B pathway (Yu et al., 2019), which is involved in oxidative stress, immune responses and inflammation in the intestine (Ma and Hottiger, 2016). Therefore, the downregulation of PAX5 and PAX9 by postbiotic LIC37 supplementation could further contribute to reducing inflammation and promoting intestinal health by modulating immune-related pathways. We also observed that both FCRLA and FCRL4 genes were downregulated by postbiotic LIC37 supplementation, which may imply that postbiotic LIC37 supplementation could potentially help modulate immune responses by reducing the expression of these Fc receptor-like family members (Bovo et al., 2024). Given that FCRLA and FCRL4 are involved in the regulation of immune function and differentiation of B cells, the downregulation of these genes might be beneficial in attenuating inflammation and potentially promoting immune homeostasis (Sohn et al., 2011; Liu et al., 2024). Specifically, FCRL4 has been shown to act as a molecular switch in B cells, inhibiting adaptive immune signaling (such as BCR signaling) while enhancing innate immune signaling (e.g., TLR9 signaling) (Sohn et al., 2011; Mahata et al., 2019). Therefore, postbiotic LIC37-induced downregulation of FCRLA and FCRL4 could contribute to a shift toward a more balanced immune response, potentially promoting a less pro-inflammatory environment and supporting intestinal health.

GO analysis provides valuable insights into gene functions, elucidating key biological processes, molecular functions, and cellular components. In the present study, we identified several GO terms associated with intestinal barrier integrity and development, including Columnar/cuboidal epithelial cell development, Negative regulation of extracellular matrix assembly, Regulation of collagen metabolic process, and Tight junction. These findings suggest that postbiotic LIC37 supplementation may reduce immune activation induced by weaning stress. Additionally, GO terms related to antioxidant capacity, such as Cellular oxidant detoxification, Glutathione metabolic process, Glutathione transferase activity, and Peroxidase activity, indicate that postbiotic LIC37 supplementation may enhance oxidative detoxification, thereby improving intestinal cell survival and reducing free radical damage. Furthermore, we identified GO terms associated with metabolic processes, including Creatine metabolic process, Creatine biosynthetic process, Regulation of phosphate transport, and Steroltransporting ATPase activity, suggesting that postbiotic LIC37 supplementation may optimize nutrient absorption through these pathways.

In the present study, we used postbiotic LIC37 to alleviate the inflammatory response in intestinal tract of calves and speculated that it would significantly affect immune response in the jejunum. We found that the DEGs were significantly enriched in the Drug metabolism - other enzymes, Vitamin digestion and absorption, Glutathione metabolism, Drug metabolism - cytochrome P450, Hepatocellular carcinoma, Chemical carcinogenesis - DNA adducts, and Metabolism of xenobiotics by cytochrome P450. Among these, Cytochrome P450-related pathways are mainly responsible for the biotransformation of exogenous compounds (Ferguson and Tyndale, 2011). Glutathione (GSH) serves as a crucial antioxidant and detoxifying molecule, playing a key role in cellular defense, heavy metal chelation, and chemical detoxification (Masella et al., 2005). Likewise, vitamins are essential for immune regulation, antioxidant protection, and energy metabolism (Pisoschi et al., 2022). Similar findings have been reported in previous research. For instance, in a transcriptome study of the ileal epithelium of lactating cows fed *Saccharomyces cerevisiae* fermentation product, significantly enrichment was also observed in Drug metabolism - other enzymes, Glutathione metabolism, and Drug metabolism - cytochrome P450 (Jiang et al., 2023). Similarly, Zhang et al. (2017) found that feeding weaned piglets with *Lactobacillus* led to significant enrichment in Arachidonic acid metabolism, Vitamin digestion and absorption, and Metabolism of xenobiotics by cytochrome P450. Consistently, our study found that dietary supplementation with postbiotic LIC37 influenced similar pathways, suggesting that postbiotic LIC37 may modulate intestinal homeostasis by regulating detoxification, oxidative stress defense, and nutrient metabolism.

5.7 Conclusion

This study demonstrates that dietary supplementation with postbiotics from heat killed *Limosilactobacillus ingluviei* C37 positively influence intestinal health in calves. Postbiotic LIC37 supplementation reduced globulin, and neutrophil levels, indicating its potential to mitigate systemic inflammation. Transcriptomic analysis revealed that postbiotic LIC37 modulates key pathways involved in nutrient metabolism, oxidative stress defense, and immune regulation by upregulating genes such as FABP1, B4GALNT2, and GSTA1, while downregulating pro-inflammatory genes like PAX5 and PAX9. These findings suggest that postbiotic LIC37 enhance intestinal barrier function, mitigate oxidative stress, and promote immune homeostasis, thereby supporting calf health during the critical weaning period. Thus, postbiotic LIC37 represent a promising and sustainable feed additive with broad applications in ruminant nutrition.

5.8 References

Aghakeshmiri, F., M. Azizzadeh, N. Farzaneh, and M. Gorjidooz. 2017. Effects of neonatal diarrhea and other conditions on subsequent productive and reproductive performance of heifer calves. **Veterinary Research Communications** 41:107-112. https://doi.org/10.1007/s11259-017-9678-9.

Amiri, S., R. Rezaei Mokarram, M. Sowti Khiabani, M. Rezazadeh Bari, and M. Alizadeh Khaledabad. 2022. Characterization of antimicrobial peptides produced by Lactobacillus acidophilus LA-5 and Bifidobacterium lactis BB-12 and their inhibitory effect against foodborne pathogens. **LWT** 153:112449. https://doi.org/10.1016/j.lwt.2021.112449.

Blake, J. A. and M. R. Ziman. 2014. Pax genes: regulators of lineage specification and progenitor cell maintenance. **Development** 141(4):737-751.

Borges, G. H., C. L. Lins-Candeiro, I. V. Henriques, R. B. de Brito Junior, M. M. Pithon, and L. R. Paranhos. 2025. Exploring the genetics, mechanisms, and therapeutic innovations in non-syndromic tooth agenesis. **Morphologie** 109(364):100941. https://doi.org/10.1016/j.morpho.2024.100941.

Bovo, S., A. Ribani, G. Schiavo, V. Taurisano, F. Bertolini, D. Fornasini, A. Frabetti, and L. Fontanesi. 2024. Genome‐wide association studies for diarrhoea outcomes identified genomic regions affecting resistance to a severe enteropathy in suckling rabbits. **Journal of Animal Breeding and Genetics** 141(3):328-342. https://doi.org/10.1111/jbg.12844.

Byrne, G., S. Ahmad‐Villiers, Z. Du, and C. McGregor. 2018. B4GALNT2 and xenotransplantation: a newly appreciated xenogeneic antigen. **Xenotransplantation** 25(5):e12394. https://doi.org/10.1111/xen.12394.

Calderón, L., K. Schindler, S. G. Malin, A. Schebesta, Q. Sun, T. Schwickert, C. Alberti, M. Fischer, M. Jaritz, H. Tagoh, A. Ebert, M. Minnich, A. Liston, L. Cochella, and M. Busslinger. 2021. Pax5 regulates B cell immunity by promoting PI3K signaling via PTEN down-regulation. **Science Immunology** 6(61):eabg5003. https://doi.org/10.1126/sciimmunol.abg5003.

CAPON, C., E. MAES, J.-C. MICHALSKI, H. LEFFLER, and Y. S. KIM. 2001. Sda-antigen-like structures carried on core 3 are prominent features of glycans from the mucin of normal human descending colon. **Biochemical Journal** 358(3):657-664. https://doi.org/10.1042/bj3580657.

Delogu, A., A. Schebesta, Q. Sun, K. Aschenbrenner, T. Perlot, and M. Busslinger. 2006. Gene repression by Pax5 in B cells is essential for blood cell homeostasis and is reversed in plasma cells. **Immunity** 24(3):269-281. https://doi.org/10.1016/j.immuni.2006.01.012.

Dusing, M. R., E. A. Maier, B. J. Aronow, and D. A. Wiginton. 2010. Onecut-2 knockout mice fail to thrive during early postnatal period and have altered patterns of gene expression in small intestine. **Physiological Genomics** 42(1):115-125. https://doi.org/10.1152/physiolgenomics.00017.2010.

Elbaz, A. M., N. K. El-Sonousy, A. S. Arafa, M. Sallam, A. Ateya, and A. Y. Abdelhady. 2024a. Oregano essential oil and Bacillus subtilis role in enhancing broiler's growth, stress indicators, intestinal integrity, and gene expression under high stocking density. **Scientific Reports** 14(1):25411. https://doi.org/10.1038/s41598-024-75533-8.

Elbaz, A. M., N. K. El-Sonousy, A. S. Arafa, M. G. Sallam, A. Ateya, and A. Y. Abdelhady. 2024b. Oregano essential oil and Bacillus subtilis role in enhancing broiler's growth, stress indicators, intestinal integrity, and gene expression under high stocking density. **Scientific Reports** 14(1):25411. https://doi.org/10.1038/s41598-024-75533-8.

Feng, C., W. Zhang, T. Zhang, Q. He, L.-Y. Kwok, Y. Tan, and H. Zhang. 2022. Heat-killed Bifidobacterium bifidum B1628 may alleviate dextran sulfate sodium-induced colitis in mice, and the anti-inflammatory effect is associated with gut microbiota modulation. **Nutrients** 14(24):5233. https://doi.org/10.3390/nu14245233.

Ferguson, C. S. and R. F. Tyndale. 2011. Cytochrome P450 enzymes in the brain: emerging evidence of biological significance. **Trends in Pharmacological Sciences** 32(12):708-714. https://doi.org/10.1016/j.tips.2011.08.005.

Fernandes, A. C., A. Reverter, K. Keogh, P. A. Alexandre, J. Afonso, J. C. P. Palhares, T. F. Cardoso, J. M. Malheiros, J. J. Bruscadin, and P. S. N. de Oliveira. 2024. Transcriptional response to an alternative diet on liver, muscle, and rumen of beef cattle. **Scientific Reports** 14(1):13682. https://doi.org/10.1038/s41598-024-63619-2.

Habashy, W. S., M. C. Milfort, A. L. Fuller, Y. A. Attia, R. Rekaya, and S. E. Aggrey. 2017. Effect of heat stress on protein utilization and nutrient transporters in meat-type chickens. **International Journal of Biometeorology** 61(12):2111-2118. https://doi.org/10.1007/s00484-017-1414-1.

Hayashi, H., S. Maruyama, M. Fukuoka, T. Kozakai, K. Nakajima, T. Onaga, and S. Kato. 2013. Fatty acid‐binding protein expression in the gastrointestinal tract of calves and cows. **Animal Science Journal** 84(1):35-41. https://doi.org/10.1111/j.1740-0929.2012.01038.x.

Hernandez, D., D. Nydam, S. Godden, L. Bristol, A. Kryzer, J. Ranum, and D. Schaefer. 2016. Brix refractometry in serum as a measure of failure of passive transfer compared to measured immunoglobulin G and total protein by refractometry in serum from dairy calves. **The Veterinary Journal** 211:82-87. https://doi.org/10.1016/j.tvjl.2015.11.004.

Izuddin, W. I., T. C. Loh, A. A. Samsudin, H. L. Foo, A. M. Humam, and N. Shazali. 2019. Effects of postbiotic supplementation on growth performance, ruminal fermentation and microbial profile, blood metabolite and GHR, IGF-1 and MCT-1 gene expression in post-weaning lambs. **BMC Veterinary Research** 15:1-10. https://doi.org/10.1186/s12917-019-2064-9.

Jiang, Q., V. Palombo, D. N. Sherlock, M. Vailati-Riboni, M. D’Andrea, I. Yoon, and J. J. Loor. 2023. Alterations in ileal transcriptomics during an intestinal barrier challenge in lactating Holstein cows fed a Saccharomyces cerevisiae fermentation product identify potential regulatory processes. **Journal of Animal Science** 101:skad277. https://doi.org/10.1093/jas/skad277.

Jin, C., S. Wu, Z. Liang, J. Zhang, X. Lei, H. Bai, G. Liang, X. Su, X. Chen, and P. Wang. 2024. Multi-omics reveal mechanisms of high enteral starch diet mediated colonic dysbiosis via microbiome-host interactions in young ruminant. **Microbiome** 12(1):38. https://doi.org/10.1186/s40168-024-01760-w.

Kelly, D. and A. Coutts. 2000. Development of digestive and immunological function in neonates: role of early nutrition. **Livestock Production Science** 66(2):161-167. https://doi.org/10.1016/S0301-6226(00)00223-2.

Kim, D., B. Langmead, and S. L. Salzberg. 2015. HISAT: a fast spliced aligner with low memory requirements. **Nature Methods** 12(4):357-360. https://doi.org/10.1038/nmeth.3317.

Kim, D. Y., B. Lim, J.-M. Kim, and D. Y. Kil. 2022. Integrated transcriptome analysis for the hepatic and jejunal mucosa tissues of broiler chickens raised under heat stress conditions. **Journal of Animal Science and Biotechnology** 13(1):79. https://doi.org/10.1186/s40104-022-00734-y.

Langmead, B. and S. L. Salzberg. 2012. Fast gapped-read alignment with Bowtie 2. **Nature Methods** 9(4):357-359. https://doi.org/10.1038/nmeth.1923.

Li, B. and C. N. Dewey. 2011. RSEM: accurate transcript quantification from RNA-Seq data with or without a reference genome. **BMC Bioinformatics** 12:1-16. https://doi.org/10.1186/1471-2105-12-323.

Liu, C., X. Li, H. Yang, X. Mao, J. Wang, and W. Gao. 2017. Effect of Natural β-Glucosidase Inhibitors in Reducing Toxicity of Amygdalin in Persicae Semen. **Phytotherapy Research** 31(5):771-777. https://doi.org/10.1002/ptr.5798.

Liu, J. p., Y. f. Jiang, J. w. Liu, C. j. Tian, Y. z. Lin, Y. z. Yang, Z. k. Zhang, Y. l. Fang, B. Huang, and H. Lin. 2024. Fc receptor-like A promotes malignant behavior in renal cell carcinoma and correlates with tumor immune infiltration. **Cancer Medicine** 13(15):e70072. https://doi.org/10.1002/cam4.70072.

Liu, N., X. Ma, X. Luo, Y. Zhang, Y. He, Z. Dai, Y. Yang, G. Wu, and Z. Wu. 2018. l-Glutamine Attenuates Apoptosis in Porcine Enterocytes by Regulating Glutathione-Related Redox Homeostasis. **The Journal of Nutrition** 148(4):526-534. https://doi.org/10.1093/jn/nxx062.

Lopes-Marques, M., C. Serrano, A. R. Cardoso, R. Salazar, S. Seixas, A. Amorim, L. Azevedo, and M. J. Prata. 2020. GBA3: a polymorphic pseudogene in humans that experienced repeated gene loss during mammalian evolution. **Scientific Reports** 10(1):11565. https://doi.org/10.1038/s41598-020-68106-y.

Lopez, A. and A. Heinrichs. 2022. Invited review: The importance of colostrum in the newborn dairy calf. **Journal of Dairy Science** 105(4):2733-2749. https://doi.org/10.3168/jds.2020-20114.

Love, M. I., W. Huber, and S. Anders. 2014. Moderated estimation of fold change and dispersion for RNA-seq data with DESeq2. **Genome Biology** 15:1-21. https://doi.org/10.1186/s13059-014-0550-8.

Ma, B. and M. O. Hottiger. 2016. Crosstalk between Wnt/β-Catenin and NF-**K**B signaling pathway during inflammation. **Frontiers in Immunology** 7:378. https://doi.org/10.3389/fimmu.2016.00378.

Mahata, S. K., W. Ying, E. M. Muntjewerff, S. Mahata, M. J. Nicolasen, S. Das, G. K. Bandyopadhyay, and G. van den Bogaart. 2019. Catestatin Improves Insulin Sensitivity by Promoting M1‑M2 Polarization and Inhibiting Obesity‑Induced Macrophage Infiltration and Gluconeogenesis in Liver. **The FASEB Journal** 33(S1):834.813-834.813. https://doi.org/10.1096/fasebj.2019.33.1_supplement.834.13.

Mahesh, M., R. K. Mohanta, and A. K. Patra. 2021. Probiotics in livestock and poultry nutrition and health. **Advances in Probiotics for Sustainable Food and Medicine** 21:149-179. https://doi.org/10.1007/978-981-15-6795-7_7.

Marteau, P. and F. Shanahan. 2003. Basic aspects and pharmacology of probiotics: an overview of pharmacokinetics, mechanisms of action and side-effects. **Best Practice & Research Clinical Gastroenterology** 17(5):725-740. https://doi.org/10.1016/S1521-6918(03)00055-6.

Masella, R., R. Di Benedetto, R. Varì, C. Filesi, and C. Giovannini. 2005. Novel mechanisms of natural antioxidant compounds in biological systems: involvement of glutathione and glutathione-related enzymes. **The Journal of Nutritional Biochemistry** 16(10):577-586. https://doi.org/10.1016/j.jnutbio.2005.05.013.

McIlwain, C. C., D. M. Townsend, and K. D. Tew. 2006. Glutathione S-transferase polymorphisms: cancer incidence and therapy. **Oncogene** 25(11):1639-1648. https://doi.org/10.1038/sj.onc.1209373.

McNeil, B., D. Renaud, M. Steele, L. Cangiano, M. Olmeda, C. Villot, E. Chevaux, J. Yu, L. Hernandez, and W. Frizzarini. 2024. Effects of weaning and inactivated

Lactobacillus helveticus supplementation on dairy calf behavioral and physiological indicators of affective state. **Journal of Dairy Science** 107(12). https://doi.org/10.3168/jds.2023-24581.

Németh, K., G. W. Plumb, J.-G. Berrin, N. Juge, R. Jacob, H. Y. Naim, G. Williamson, D. M. Swallow, and P. A. Kroon. 2003. Deglycosylation by small intestinal epithelial cell β-glucosidases is a critical step in the absorption and metabolism of dietary flavonoid glycosides in humans. **European Journal of Nutrition** 42(1):29-42. https://doi.org/10.1007/s00394-003-0397-3.

Pisoschi, A. M., A. Pop, F. Iordache, L. Stanca, O. I. Geicu, L. Bilteanu, and A. I. Serban. 2022. Antioxidant, anti-inflammatory and immunomodulatory roles of vitamins in COVID-19 therapy. **European Journal of Medicinal Chemistry** 232:114175. https://doi.org/10.1016/j.ejmech.2022.114175.

Reuben, R. C., P. C. Roy, S. L. Sarkar, A. S. M. Rubayet Ul Alam, and I. K. Jahid. 2020. Characterization and evaluation of lactic acid bacteria from indigenous raw milk for potential probiotic properties. **Journal of Dairy Science** 103(2):1223-1237. https://doi.org/10.3168/jds.2019-17092.

Rodrigo, I., R. E. Hill, R. Balling, A. Münsterberg, and K. Imai. 2003. Pax1 and Pax9 activate Bapx1 to induce chondrogenic differentiation in the sclerotome. **Development** 130(3):473–482. https://doi.org/10.1242/dev.00240.

Romero, L., K. Andrews, L. Ng, K. O'Rourke, A. Maslen, and G. Kirby. 2006. Human GSTA1-1 reduces c-Jun N-terminal kinase signalling and apoptosis in Caco-2 cells. **Biochemical Journal** 400(1):135-141. https://doi.org/10.1042/BJ20060110.

Salminen, S., M. C. Collado, A. Endo, C. Hill, S. Lebeer, E. M. Quigley, M. E. Sanders, R. Shamir, J. R. Swann, and H. Szajewska. 2021. The International Scientific Association of Probiotics and Prebiotics (ISAPP) consensus statement on the definition and scope of postbiotics. **Nature Reviews Gastroenterology & Hepatology** 18(9):649-667. https://doi.org/10.1038/s41575-021-00440-6.

Sharma, R., Y. Yang, A. Sharma, S. Awasthi, and Y. C. Awasthi. 2004. Antioxidant role of glutathione S-transferases: protection against oxidant toxicity and regulation of stress-mediated apoptosis. **Antioxidants and Redox Signaling** 6(2):289-300. https://doi.org/10.1089/152308604322899350.

Sirisopapong, M., T. Shimosato, S. Okrathok, and S. Khempaka. 2023. Assessment of lactic acid bacteria isolated from the chicken digestive tract for potential use as poultry probiotics. **Animal Bioscience** 36(8):1209. https://doi.org/10.5713/ab.22.0455.

Sohn, H. W., P. D. Krueger, R. S. Davis, and S. K. Pierce. 2011. FcRL4 acts as an adaptive to innate molecular switch dampening BCR signaling and enhancing TLR signaling. **Blood, The Journal of the American Society of Hematology** 118(24):6332-6341. https://doi.org/10.1182/blood-2011-05-353102.

Song, Y., H. Sun, Z. He, A. Fischer-Tlustos, T. Ma, M. Steele, and L. L. Guan. 2021. Transcriptome analysis revealed that delaying first colostrum feeding postponed ileum immune system development of neonatal calves. **Genomics** 113(6):4116-4125. https://doi.org/10.1016/j.ygeno.2021.10.011.

Thorsteinsson, M. M., N. Canibe, and M. Vestergaard. 2020. Effect of dietary supplementation of Saccharomyces cerevisiae and a postbiotic from Lactobacillus acidophilus on the concentration of organic acids, biogenic amines, and microbiota in the small intestine and colon of rosé veal calves. **Journal of Animal and Feed Sciences** 29(4):345-351. https://doi.org/10.22358/jafs/131078/2020.

Tsukagoshi, M., M. Sirisopapong, F. Namai, M. Ishida, S. Okrathok, S. Shigemori, T. Ogita, T. Sato, S. Khempaka, and T. Shimosato. 2020. Lactobacillus ingluviei C37 from chicken inhibits inflammation in LPS‐stimulated mouse macrophages. **Animal Science Journal** 91(1):e13436. https://doi.org/10.1111/asj.13436.

Van Niekerk, J., M. Middeldorp, L. Guan, and M. Steele. 2021. Preweaning to postweaning rumen papillae structural growth, ruminal fermentation characteristics, and acute-phase proteins in calves. **Journal of Dairy Science** 104(3):3632-3645. https://doi.org/10.3168/jds.2020-19003.

Vasiee, A., F. Falah, B. A. Behbahani, and F. Tabatabaee-yazdi. 2020. Probiotic characterization of Pediococcus strains isolated from Iranian cereal-dairy fermented product: Interaction with pathogenic bacteria and the enteric cell line Caco-2. **Journal of Bioscience and Bioengineering** 130(5):471-479. https://doi.org/ 10.1016/j.jbiosc.2020.07.002.

Wang, B., L. Gong, Y. Zhou, L. Tang, Z. Zeng, Q. Wang, P. Zou, D. Yu, and W. Li. 2021. Probiotic Paenibacillus polymyxa 10 and Lactobacillus plantarum 16 enhance growth performance of broilers by improving the intestinal health. **Animal Nutrition** 7(3):829-840. https://doi.org/10.1016/j.aninu.2021.03.008.

Wang, G., H. L. Bonkovsky, A. de Lemos, and F. J. Burczynski. 2015. Recent insights into the biological functions of liver fatty acid binding protein 1. **Journal of Lipid Research** 56(12):2238-2247. https://doi.org/10.1194/jlr.R056705.

Yan, J., Y. Gong, Y.-M. She, G. Wang, M. S. Roberts, and F. J. Burczynski. 2009. Molecular mechanism of recombinant liver fatty acid binding protein's antioxidant activity. **Journal of Lipid Research** 50(12):2445-2454. https://doi.org/10.1194/jlr.M900177-JLR200.

Yang, Y., J.-Z. Cheng, S. S. Singhal, M. Saini, U. Pandya, S. Awasthi, and Y. C. Awasthi. 2001. Role of glutathione S-transferases in protection against lipid peroxidation: overexpression of hGSTA2-2 in K562 cells protects against hydrogen peroxide-induced apoptosis and inhibits JNK and caspase 3 activation. **Journal of Biological Chemistry** 276(22):19220-19230. https://doi.org/10.1074/jbc.M100551200.

Yu, J., D. Li, and H. Jiang. 2020. Emerging role of ONECUT2 in tumors. **Oncology Letters** 20(6):328. https://doi.org/10.3892/ol.2020.12192.

Yu, M., S. W. Wong, D. Han, and T. Cai. 2019. Genetic analysis: Wnt and other pathways in nonsyndromic tooth agenesis. **Oral Diseases** 25(3):646-651. https://doi.org/10.1111/odi.12931.

Zhang, D., T. Shang, Y. Huang, S. Wang, H. Liu, J. Wang, Y. Wang, H. Ji, and R. Zhang. 2017. Gene expression profile changes in the jejunum of weaned piglets after oral administration of Lactobacillus or an antibiotic. **Scientific Reports** 7(1):15816. https://doi.org/10.1038/s41598-017-16158-y.

Zhang, L., C. Li, X. Song, R. Guo, W. Zhao, C. Liu, X. Chen, Q. Song, B. Wu, and N. Deng. 2024. Targeting ONECUT2 inhibits tumor angiogenesis via down-regulating ZKSCAN3/VEGFA. **Biochemical Pharmacology** 225:116315. https://doi.org/10.1016/j.bcp.2024.116315.

Zhao, K., Y. Chen, G. Penner, M. Oba, and L. Guan. 2017. Transcriptome analysis of ruminal epithelia revealed potential regulatory mechanisms involved in host adaptation to gradual high fermentable dietary transition in beef cattle. **BMC Genomics** 18:1-17. https://doi.org/10.1186/s12864-017-4317-y.